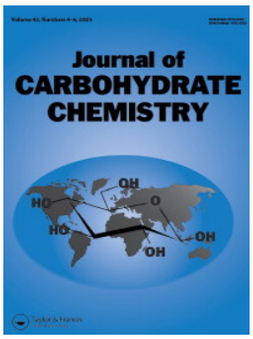

Taylor & Francis
Taylor & Francis Group

Journal of Carbohydrate Chemistry

ISSN: (Print) (Online) Journal homepage: www.tandfonline.com/journals/lcar20

Chemically modified starch with silicon quantum dots: Structures and properties

Filiz Saman, Ebru Al, Bilge Boylu & Osman Arslan

To cite this article: Filiz Saman, Ebru Al, Bilge Boylu & Osman Arslan (2023) Chemically modified starch with silicon quantum dots: Structures and properties, Journal of Carbohydrate Chemistry, 42:4-6, 158-179, DOI: 10.1080/07328303.2024.2315529

To link to this article: https://doi.org/10.1080/07328303.2024.2315529

JOURNAL OF CARBOHYDRATE CHEMISTRY
2023, VOL. 42, NOS. 4–6, 158–179
https://doi.org/10.1080/07328303.2024.2315529

Taylor & Francis
Taylor & Francis Group

Chemically modified starch with silicon quantum dots: Structures and properties

Filiz Saman, Ebru Al, Bilge Boylu, and Osman Arslan

Food Engineering Department, İstanbul Sabahattin Zaim University, Istanbul, Turkey

ABSTRACT

Attachment of Silicon quantum dots (Si QDs) onto starch via sol-gel controlled covalent bonding to form hybrid starch particles was developed to modulate the optical, physical, and mechanical features of starch. Fabricated Si QDs chemically interacted with –OH side groups due to the sol-gel reactions on the starch molecules providing a detectable new molecular bonding to result in fluorescent emission. The produced structures formed nonlinear morphological orientations that provide a nanocomposite material platform for a facile molecular marking in daily applications.

GRAPHICAL ABSTRACT

Fluorescent tag attachment onto the starch structures by Si quantum dots via covalent bonding was developed for the varying implications including fluorescent materials, sensors, surface coating purposes. A well designed quantum dot synthesis and starch treatment was applied to vary the optical, physical, and mechanical features of the starch particles on molecular level resulting a promising new material for visible light fluorescent material applications.

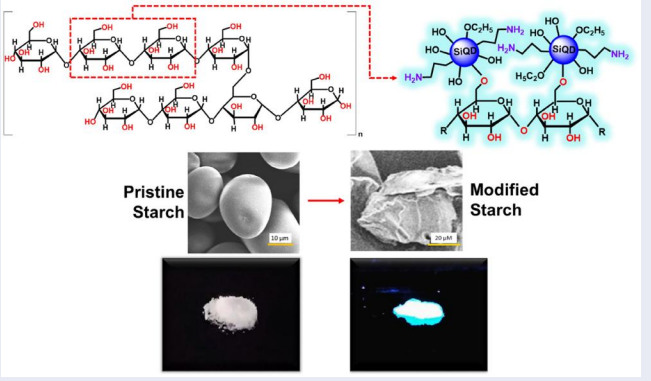

ARTICLE HISTORY
Received 20 March 2023
Accepted 22 January 2024

KEYWORDS
Fluorescent barcode; functional coating; nanocomposite; quantum dot; starch modification

CONTACT Osman Arslan o.arslan@izu.edu.tr Food Engineering Department, İstanbul Sabahattin Zaim University, 34303 Istanbul, Turkey.

Supplemental data for this article can be accessed online at https://doi.org/10.1080/07328303.2024.2315529.
This article was originally published with errors, which have now been corrected in the online version. Please see Correction (http://dx.doi.org/10.1080/07328303.2024.2328417)

Introduction

Starch is commonly applied to food, paper, adhesive, oil, and textile industries.[1–3] Especially in the food industry, apart from its use as a new material, starch is utilized as a thickener, gelling and shaping agents due to its viscosity properties[4] and as encapsulation agent of flavor[5] and nutraceuticals.[6] Potato starch is also used in paper[7] and adhesive products due to its binding power[8,9] and the oil industry[10] for its functional features. Generally, potato starch swells liquids more easily than cereal starches.[11,12] Natural starch granules can slightly swell reversibly in cold water but are insoluble, while in hot water, swelling occurs irreversibly with gelatinization.[13] The starch structure consists of ca. 20% amylose and 80% amylopectin.[14] It is tasteless, white in color, and powder in macroscopic form.[15]

Modified starches can be obtained by many methods and are useful due to their rheological, esthetic, sensory, functional, and nutritional properties.[16,17] The modification methods can be classified as physical, chemical, genetic, and enzymatic modifications.[18] Physical modification reflects the safest way of modification for the food industry since it does not modify the material profoundly and has a vast varieties such as thermal inhibition,[19] pulsed electric field effect, microwave,[20] and osmotic pressure treatment.[21] Related materials and nanotechnology have been utilized to add constructive features such as appearance, shelf life, nutritional value, taste, and texture to foods or to protect and maintain the features of different materials.[22–24]

In literature, many examples for Silicon quantum dot (Si QD) synthesis by reducing methods using agents such as sodium ascorbate,[25] ascorbic acid (AA),[26] glucose,[27] citric acid,[28] and chitosan[29] are available. Studies reveal that the fluorescence origin of Si QDs is quantum size effect of Si (particle size-dependent properties caused by the discrete energy states), indicated by the X-ray diffraction (XRD) patterns of Silicon crystals.[30–33] In addition, fluorescent silicon/silica-based nanoparticles (NPs) derived from 3-(aminopropyl)triethoxysilane (APTES) and AA under a nitrogen atmosphere contain the Si core, which is responsible for luminescence origin. QD and starch interactions have been reported, for example, for QD detection of starch,[34] fluorescent graphene QD preparation,[35] starch ligand stabilization for QDs,[36] and QD decoration for composite structures.[37] Moreover, metal complexes of starch[38] and various carbon QDs are available in the literature for different applications.[39–41] In this research, we attempt to synthesize light emitting starches for (a) Si QD and starch nanocomposite formation, (b) new light emitting material applications, and (c) investigation of the geometrical and chemical variations of starch. Our results showed that it is technically possible to prepare Si QD

and chemically attach them to starch as new light emitting QD-modified fluorescent materials.

Results and discussion

Synthesis and characterization of Si QDs and Si QD-modified starch

The Si QDs were synthesized by reactions of the silicon precursor with sodium ascorbate in an aqueous environment using characterized electromagnetic radiation. Two solutions of different precursor concentrations in total volumes of 20 and 40 mL were tested to produce Si QDs. For example, the irradiation time for the 40 mL solution, which had a lower precursor concentration compared to the 20 ml solution, was 45 min to obtain stable results of Si QD production. Figure 1 shows the Si QD synthesis method and fluorescence emission results. Transmission electron microscopy (TEM) and high resolution (HR)-TEM results for both Si QDs (Supplementary Fig. S1) show their modified and controlled surface features, having monodisperse character and small nanocrystal sizes (20 mL Si QD = 2.2 nm, and 40 mL Si QD = 2.0 nm) of spherical shape. The HR-TEM image (Supplementary Fig. S1) also shows the high crystallinity of the Si QD lattice fringes with 0.30 nm interplanar spacing for both, consistent with the (111) plane of diamond Si. Optical investigations revealed the Ultraviolet-visible (UV-Vis) absorption (Supplementary Fig. S1) characteristics of Si QD and proved their size-selective absorption.

To produce modified starch, Si QD was chemically attached to starch (Fig. 2). Si QD solutions reacted with starch powder under the sol-gel reaction condition as listed Supporting Table S1. As mentioned before, there are many methods to synthesize Si QDs through reduction.[25–29] Especially, chitosan and glucose reduction unveil straightforward Si nanoparticle synthesis. Glucose plays dual roles as reducing agent and hydrophilic ligands for the production of silicon nanoparticles (SiNPs), having both Si–O and Si–Si bindings in their lattice structure and pseudo-glucose moieties at their surface. Low molecular weight chitosan was also used as a reducing agent for Si QD synthesis from APTES. Due to their photoluminescent properties, SiNPs can be used as fluorescent probes, solar cells, down-shifting coatings, and biosensors. It was claimed that the nano platform has a core-shell structure in which the chitosan is on the surface. In our study, a detailed analysis of the visual pictures of the Si QD solutions unveils that the yellowish-orange solution emits bright green lights for all timelines with proper excitation. Analysis showed that the modified Si-QDs, which are composed of a crystalline silicon core and a possible silica shell due to the sol-gel reactions, have aminopropyl, alkoxide ($-OC_2H_5$), and –OH groups to provide water-soluble QDs.

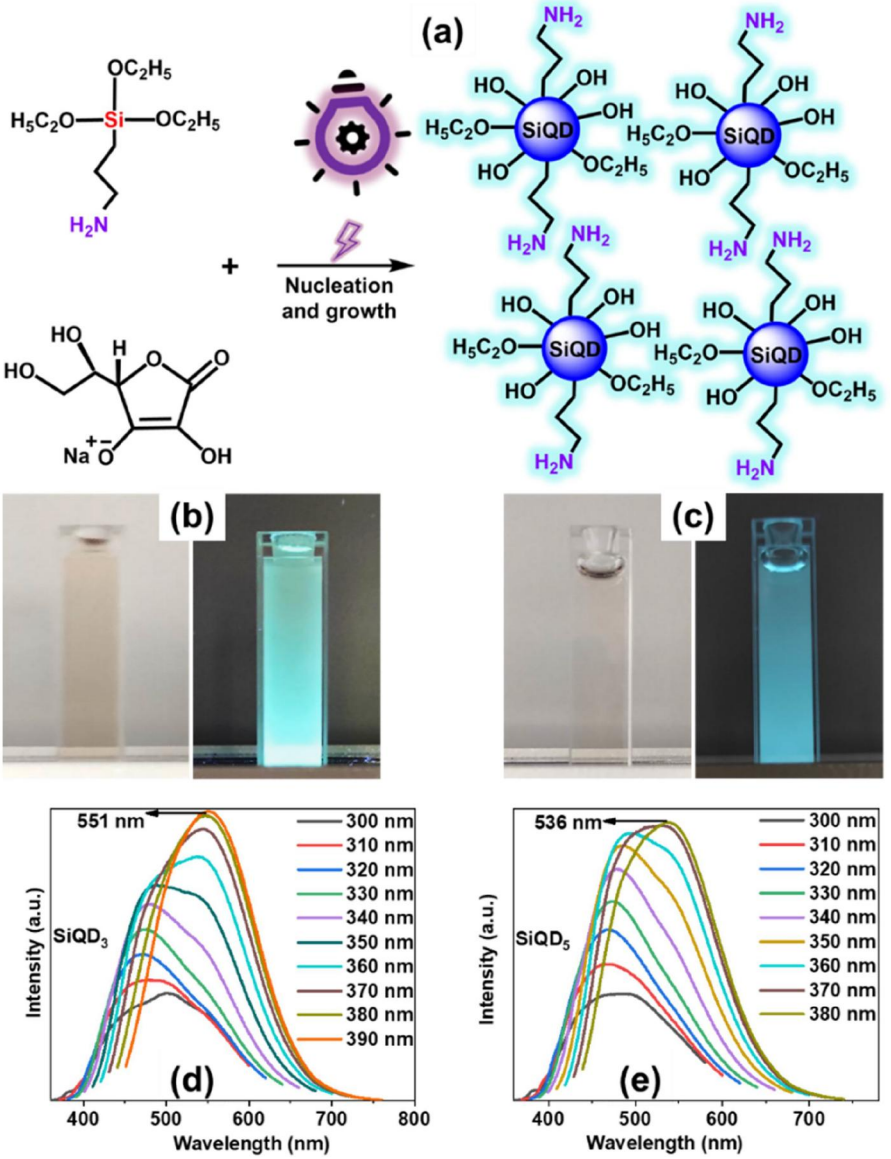

Figure 1. (a) Fabrication of Si QDs by UV irradiation method; (b) visible emission features of Si QDs derived from higher concentration of precursor under daylight and UV excitation; (c) visible emission features of Si QDs derived from lower concentration of precursor under daylight and UV excitation; (d) photoluminescence (PL) graphics with varying excitation wavelengths for b; (e) PL graphics with varying excitation wavelengths for c.

Visible light emission properties are related to the quantum confinement effect due to the size of the Si QD with controlled surface groups. From the solutions of both Si QDs, visible emission was detected between 480 and 550 nm with varying excitations between 300 and 400 nm, respectively. Generally, chemical cross-linking (Fig. 2) plays an important role in varying

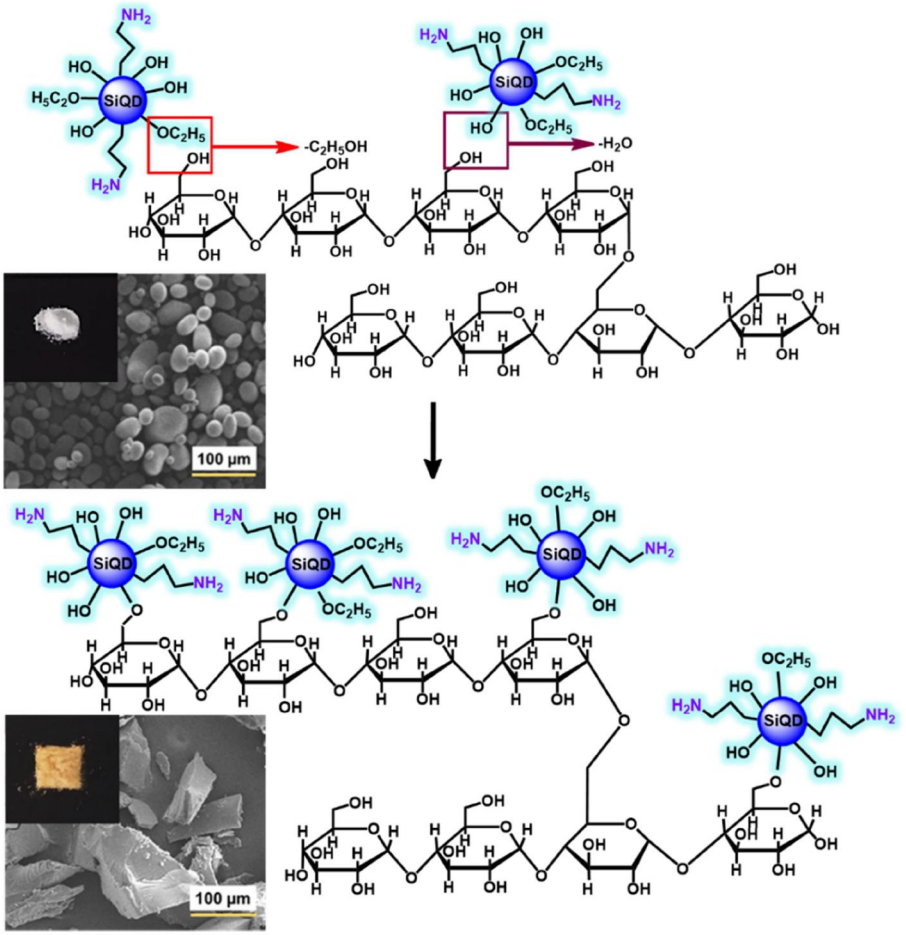

Figure 2. Chemical attachment of Si QD onto starch and the scanning electron microscopy (SEM) images of starch and the modified starch with daylight appearance (insets).

the physical and chemical properties of the native starch, such as solubility, thermal properties, and reaction capability. It is reported that cross-linked starch is a promising multifunctional reagent that allows polymeric interactions, diverse food applications, and other applications. Therefore, the detection of the surface modification of the starch is vitally important for future applications. From the perspective of the effect of Si QD concentration on starch, modification was studied. Increased amounts of Si QD were used to modify the same quantities of starch. According to the results of thermogravimetric analysis (Fig. 3) using Si QD-modified products F1, F2, and F3, it is clear that increasing amounts of Si QD provided increasing Si QD modifications. Thermogravimetric analysis (TGA, in Fig. 3(a,b)) show that pristine starch decomposes at four different steps, if we simply ignore the small variations.

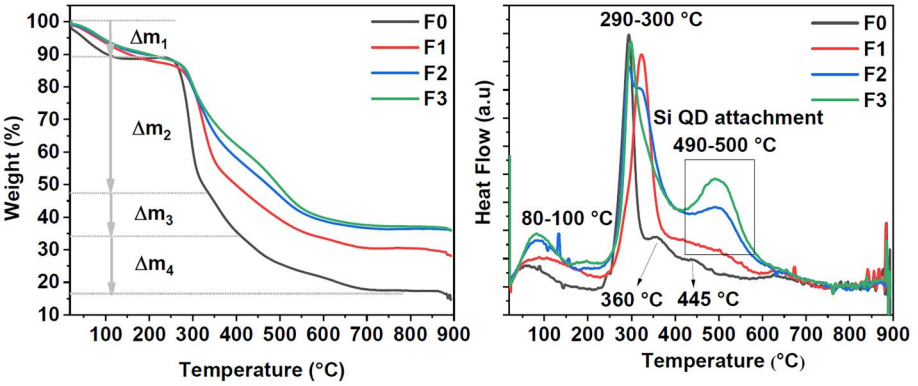

Figure 3. (a) Thermogravimetric comparison of the pristine and Si QD-modified starch F1, F2, F3 with increasing Si QD; (b) differential thermal analysis (DTA) graphs of the pristine and Si QD-modified starch F1, F2, F3 with increasing Si QD.

In TGA, a total of 87% mass loss was measured in DTA. This amount of loss is proper for the pristine potato starch, as reported in the literature, with slight variations since other types of starch have different levels of branches and different mass losses[42] DTA (Fig. 3(b)) has also revealed that the first loss appears at around 80–100 °C, second at 290–300 °C, and the third at 360 °C. The last broad and slight DTA peak appears at 445 °C. Strikingly, increasing the amount of Si QD for starch modification resulted in thermal loss decreases to 72% for F1, 65% for F2, and 62% for F3, respectively.

While this investigation has confirmed the attachment of Si QD onto starch, analyses were also made (Supplementary Fig. S2) for F9, F15, and F24, respectively. For F9, the thermal loss was 64%, and it was 67% for F15 and 84% for F24, respectively. Since the Si QD amount was relatively low in the F24 sample (50 times diluted when compared to F15), it was concluded that even 1–3% amount of Si QD is enough for the modification and fluorescence transfer to the starch for nanomaterial applications. Thermal loss temperatures and decomposition shapes are similar, allowing the conclusion that Si QD modification is only changing its loss amount in the same manner. After the modification (F1, F2, F3), a new peak arising at 490–500 °C is clear evidence of the SiQD attachment onto the pristine starch molecules.

Si QD attachment can also be detected by the comparison of atomic mapping of pristine starch and F24 as presented in Figure 4. Atomic mapping of the pristine starch and other modified structures (e.g., F9 and F15) were also presented (Supplementary Fig. S3). First scanning electron microscopy (SEM) images of the samples were templated, and Si, C, N, O mapping results were successfully investigated. The results show that no noticeable N and Si mapping pattern is available in the pristine starch. At

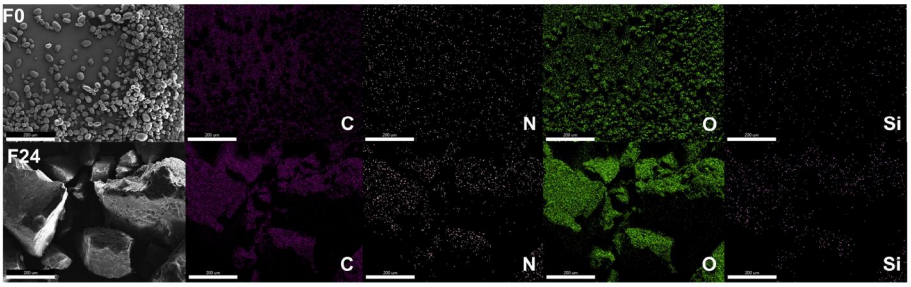

Figure 4. Atomic mapping analysis of pristine starch and Si QD-modified samples as F24.

the same time, all four elements can be detected clearly in other Si QD-modified samples. Since N (nitrogen) is relatively low in all samples, mapping templates hardly unveil the particle shapes. However, for trustable results, the count rate and mapping time of the process were enhanced. During mapping, quantitative EDX (energy dispersive X-Ray) measurements were also conducted, which is compatible with XPS (X-Ray photoelectron spectroscopy) and SEM -EDX results (Supplementary Table S2).

A series of techniques with varied concentrations of Si characteristics in the final material was applied for modifications of starch with Si QD. Therefore, pristine starch was compared with F9 and F15. The results showed that a slight yellowish color for the Si QD modification might cause a visual side effect. The perfectly white Si QD-modified starch F24 sample was also investigated. Firstly, SEM features (Fig. 5) and physical variations were analyzed. The crystalline features of these four samples unveil a detectable change in crystallinity with a hybrid crystalline structure formation. Modification of the starch surfaces reveals profound variations when compared to pristine starch according to the SEM images (Fig. 5). Generally, if there is no substantial modification, smooth surfaces of the pristine starch with cracks or holes are observed. However, in this type of modification, the shape, smoothness, size, and specific surface area of starch might not be affected. According to the SEM images of pristine starch, uneven shape and size are observable with flat surfaces. No pores, no cracks, or even wrinkles are observed. Size analysis was given together with that of other modified examples F9, F15, and F24 in Supplementary Figure S4. Results revealed that after the Si QD modification, irregularly shaped new starch structures with new crystallinity were observed. Sizes of the Si QD-modified starch are always greater than pristine starch. Pristine starch generally has a 16-micron diameter and 22-micron length. The length was increased to 172 µm for F9 and 222 µm for F15, while interestingly, low concentration F24 was 293 µm. SEM images of the apparent and layered structures of Si QD-modified starch support the statistical analysis. EDX analysis (Supplementary Table S2) also revealed that for each sample

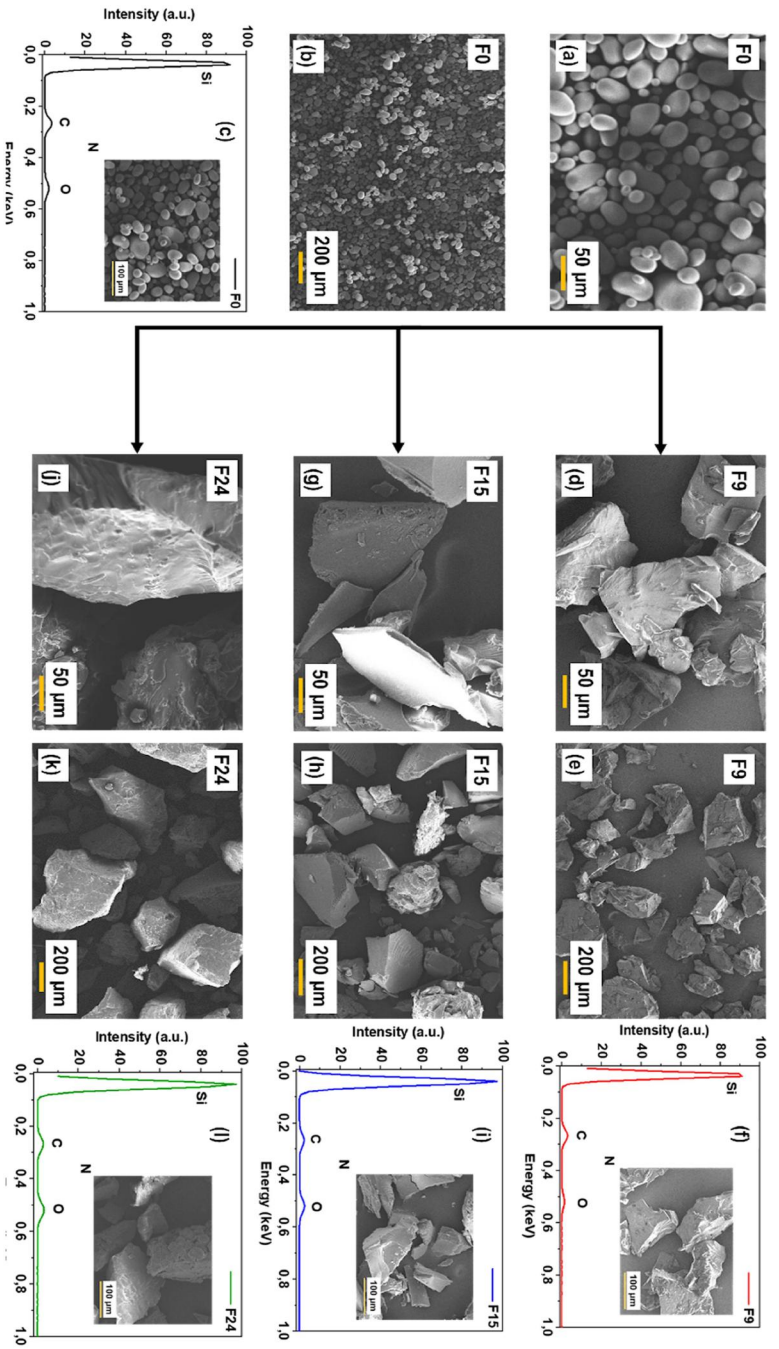

Figure 5. SEM and EDX investigation of the pristine and Si QD modified starch structures; SEM images of pristine starch with enlarged (a) 91 X (b) 410 X form (c) EDX graph of the pristine starch (SEM image of the same as inset), (d) SEM image of F9 with 98 X enlargement (e) SEM image of F9 with 403 X enlargement (f) EDX graph of the F9 (SEM image of the same as inset) (g) SEM image of F15 with 84 X enlargement (h) SEM image of F15 with 412 X enlargement (i) EDX graph of the F15 (SEM image of the same as inset) (j)SEM image of F24 with 86 X enlargement (k) SEM image of F24 with 411 X enlargement (l) EDX graph of the F24 (SEM image of the same as inset).

of F0 (pristine starch), F9, F15, and F24, modified structures contain Si atoms with relatively increasing order, while pristine starch shows no similar result.[43]

In conclusion, TEM and UV-Vis investigations have clearly proven the Si QD formation, and additionally, SEM, TG-DTA, and EDX analysis, together with atomic mapping, evidently confirmed the molecular attachment of the Si QD to starch. Thus, these results clearly confirmed that Si QD extensively modified the surface of starch and changed the geometrical orientation of its original structure.

Crystallinity and surface analysis of the chemically modified starch

Comprehensive XRD analysis confirmed that the treatment does not cause full dissolution or collapse, but layered granules were formed. For example, XRD results (Fig. 6) showed that pristine starch and the modified derivatives have semicrystalline structures with some amorphous features. Due to modification, additional peaks were observed, especially in low-concentration Si QD-modified F24. Higher diffraction intensity with varying Si QD modification showed a higher degree of crystallinity when compared to pristine starch. It is widely known that starch has three different crystalline structures, type A, type B and type C, which is a mixture of A + B. In the A-type structure, different peak intensities for 2θ angles of refraction at 15°, 17°, 18°, and 23° are available. Interestingly B-type also contains angles of refraction for 2θ at 5°, 6°, 15°, 17°, 22°, and 23°, and this is more prominent in tuberous starches. As expected, C-type is a blend of types A and B. Based on the investigation, pristine starch shows the B-type crystallinity with angles of refraction for 2θ at 15°, 17°, 22°, and 23° and mostly preserves its character for F9 with peak angle at 18–19°. This result clearly shows that Si QD modification causes the formation of A-type crystallinity with existing predominant B-type crystallinity.

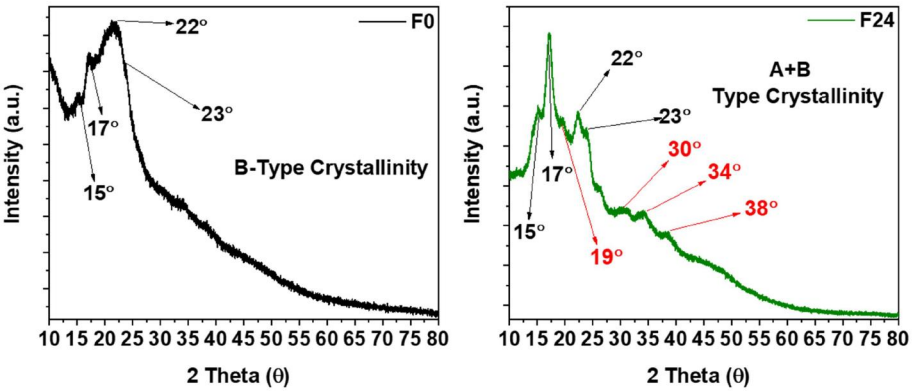

Figure 6. XRD diffractograms of the pristine (F0) starch and Si QD-modified (F24) starch.

It is known that the polymerization degree of the branched chains of amylopectin is related to the type of polymorphism, and B-type starches typically exhibit a large portion of long-chain (DP > 37).[44] When observed in Si QD-modified structures, a pattern of crystallinity of mostly C-type tuber structure with major peaks for 2θ at 15°, 17°, 22°, and 23° is expected. Thermal treatment reduces typically diffraction densities and lower the peak intensities like in cooked starch. Nevertheless, Si QD-modified starch with 80 °C treatment shows similar behavior. The expected amorphous structure was not detected after the modifications, and interestingly new peaks arose, as presented in F9 and F15 (Supplementary Fig. S5). Some other XRD investigations conducted for F2, F8, F10, and F17 also supported the idea of type A + B crystalline formation of starch after Si QD modification (Supplementary Fig. S5).

Fourier transformed-Infrared spectroscopy (FT-IR) analysis (Supplementary Fig. S6) of the modified starch also highlights the molecular variations compared to pristine starch. It is known that FT-IR of the commercial starch shows analog peaks at around 3,300, 2,930, and 1,650 cm^{-1}. Especially, peaks at 1,650 cm^{-1} can be assigned to water molecules absorbed in the starch, where typically stretching vibration of the carbonyl (C=O) band appears. In this study, peaks at 1,646 cm^{-1} were observed in pristine starch. Usually when available, the peak at 2,100 cm^{-1} originates from free water, and peaks at 2,930 and 3,300 cm^{-1} are due to -CH_2 deformation and the –OH bonds, respectively. An increasing amount of Si QD modification in F1, F2, and F3 causes new peaks in 1,560 and 1,145 cm^{-1} due to the Si–O bond, which are absent in pristine starch. Especially, Si–O bonds and C-H variations were detected and labeled in the FT-IR spectrums, inclining the attachment of Si QD (Supplementary Fig. S6). Results also unveiled that, with increasing amount of Si QD modification, the –OH functional group intensity of the pristine starch decreased. Additionally, C–O peaks arise around 1,000 and 1,200 cm^{-1} and show some variations with modification.[45] NH_2 groups on the Si QD do not appear clearly as they have generally positioned after 3,000 cm^{-1} even though atomic mapping detected N atom in the scans. General C-H peaks were detected at 2,854 cm^{-1}, originating from the precursor compound. The fingerprint region peaks at 690 and 759 cm^{-1}, possibly related to Si–O bonding. After the sol-gel reaction, these peaks are naturally expected since a silica shell must be formed around the Si QD. All F9, F15, and F24 samples exhibit the mentioned FT-IR peaks, showing similar features of Si QD.

For the surface mapping and the comparison of the starch surface before and after the Si QD modification, XPS (Fig. 7) was applied. For the pristine starch, since C and O are the only atoms detected by the survey and high-resolution XPS techniques, they were set as the prominent peak positions

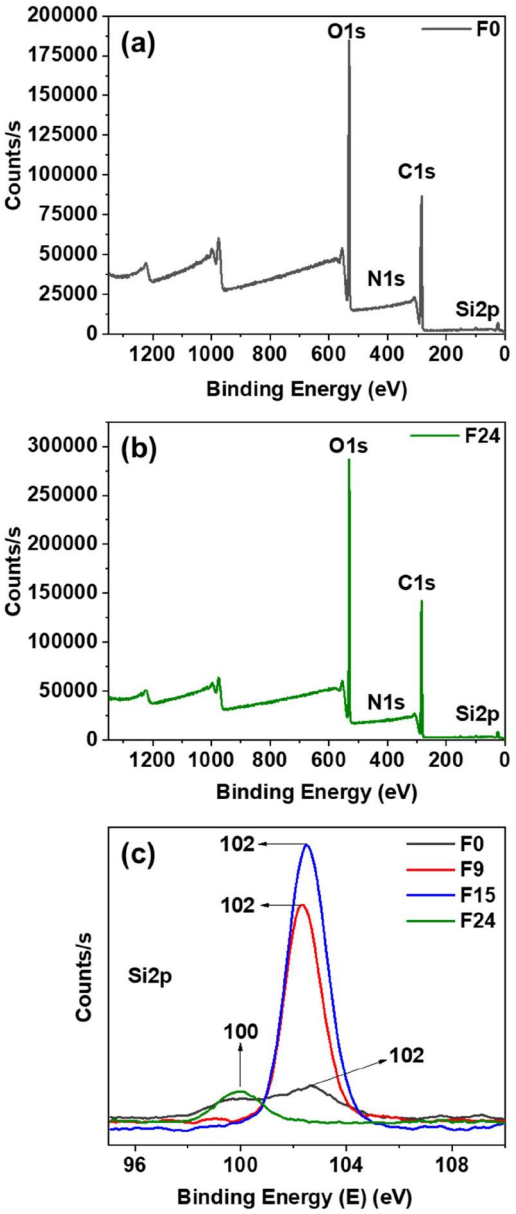

Figure 7. Survey XPS spectra of the (a) pristine starch F0 and (b) F24 together with high resolution overlapped, (c) Si 2p HR-XPS spectra of the pristine starch F0 and Si QD-modified F9, F15 and F24 starches.

for the measured pristine and modified starch values for detecting the Si QD attachment. Figure 7 represents the survey XPS spectra of the pristine starch together with F9, F15, and F24. A general look reveals that modified samples contain Si 2p peaks where pristine starch has no sign of this peak, claiming a successful modification process. Detection of the Si 2p peak is a facile and effective method for detecting Si QD modification on starch

molecules (Supplementary Fig. S7). Atomic compositions of pristine and the three modified samples were also presented in Supplementary Table S2to confirm that increasing Si QD loading can also be detected by increasing atomic percentages.

When survey spectra of the pristine and Si QD-modified samples F9, F15, and F24 were analyzed, a relatively high O 1s peak was observed in the pristine starch, which appears lower in the F9 sample. F9 intensity variation for O 1s is the complete coverage and concentration of the Si QD-modified cation in solution. Since the sol-gel reaction governs the surface and allows the interaction between Si QD and the starch surface, the oxygen amount is reduced. Still, O 1s peaks for F15 and F24 appear as the highest peak in the survey spectra. Since Si QD contains $-NH_2$ peaks, it is also possible to find N 1s peaks at modified samples at around 399.5–400.0 eV (not shown). When HR-XPS peaks were analyzed, remarkable results were observed for the pristine and modified starch structures. HR-XPS results (Fig. 7(c)) stress that 102.4 eV value was detected for Si 2p peak when the F9 sample was investigated. Similarly, 102.5 eV was detected for F15, and low Si QD concentration F24 reflected a 100.2 eV value. The irregularly shaped peak does not represent the Si 2p peak for the pristine starch sample. Therefore, as expected, one can easily track the Si QD concentration attached to starch molecules by XPS spectroscopy. Quantitative amounts of Si QD attached in F9, F15, and F24 were also presented in Supplementary Table S2 employing Si 2p peaks intensity. Since the sol-gel method is the main route for producing Si QD, additional alkoxide and –OH groups are available in Si QD solution before the attachment. This detail can be confirmed by facile attachment via –OR and –OH condensation, which transfers the fluorescence features of the Si QD onto modified starch. C 1s HR-XPS peaks of pristine starch and modified F9, F15, and F24 starches revealed that the C 1s peak for pristine starch has the value of 285.1 eV, and its deconvolution reveals two different carbon types, which is compatible with literature results.[46] After Si QD modification, the central peak of C 1s remained the same at 285.0 eV. However, two additional peaks appeared in deconvolution analysis at 287.7 and 289.6 eV, confirming the changing chemical environment of the starch structures after Si QD modification. Similar analysis revealed 285.2, 286.4, and 288.3 eV for C 1s peaks for the modified F15 sample. Interestingly, for F24, C 1s peaks resulted from 284.2 eV as the prominent peak and 282.1 eV as the satellite peak, possibly due to the low Si QD concentration. O 1s peaks for pristine starch and modified samples reflected behaviors like carbon XPS peaks. While pristine starch O 1s peak was mainly positioned on 530.0 eV, F9 was mainly positioned at 532.5 eV and another at 534.2 eV detected by deconvolution. F15 O 1s peaks shift to 532.7 eV, and lastly, F24 peaks are seen at

530.8 eV. Thus, Si QD modification on a starch structure can be observed by XPS investigation as survey and high-resolution peaks revealed the necessary atomic interactions.

Nanocomposite applications of the chemically modified starch

Using starch as a reinforcement agent is an effective method for improving film properties or enhancing structural endurance. Especially, the nanocrystal/nanoparticle form of starch acts as a reinforcing agent to generate nanocomposites with improved features. The main advantage of this phenomenon is due to the –OH groups available on the surface of the nanoparticles. Every single modification method mainly targets a small portion of the starch structure. Even after harsh modification techniques, some –OH groups are still present, providing further interaction with other molecules. Some results showed increased surface roughness with increased incorporation of starch in the oxidized form and improved mechanical properties. Si QD-modified starch was used to produce fluorescent selective nanocomposite coating materials by sol-gel method (Fig. 8). To this end, commercial 3-glycidyloxypropyl trimethoxy silane (GPTMS) was used to react with aluminum tri-seconder butoxide [$Al(OsBu)_3$]. Ethyl acetoacetate was used as a complexing ligand for $Al(OsBu)_3$ to control its reactivity. F9 was added (5%) into hydrolyzed GPTMS, and dispersion was performed without dispersing glass balls for the hybrid nanocomposite coatings. Coating solutions were performed on selective surfaces of 10×10 cm glass substrates, which were applied by a spray coating method. GPTMS was hydrolyzed by acidic (HCl) water solution and hydrolysis-condensation reactions of epoxy silane. After adding Si QD-modified starch, the solution was monitored for the production of a hybrid nanocomposite coating.[47,48] Flow chart for the procedure of coating production is presented in Figure 8. Prehydrolized epoxy silane with Si QD-modified starch was dispersed by adding acidic water to complete the hydrolysis of remaining –OR groups, and dispersion was conducted around 2.5 h. After the dispersion chelated, aluminum co-reactant was added, and the whole solution was stirred vigorously for 10–15 min; the milky solution was applied to a glass substrate by spray method.

SEM (Fig. 9(a)), FT-IR polymerization (Fig. 9(b)), and emission features (Fig. 9(c)) of select nanocomposite fluorescent coatings were analyzed. FT-IR showed –OH peaks at around 3,300 cm^{-1} possibly arising from pre-hydrolyzed GPTMS and also from precursor $Al(acaOEt)(OsBu)_2$. Additionally, the aluminum complex has a carbonyl group at 1,610 and 1,524 cm^{-1}, respectively. An epoxy group that provides a polymeric opening and ethylene oxide repeating structure at 906 cm^{-1}, successfully polymerized at the same position,

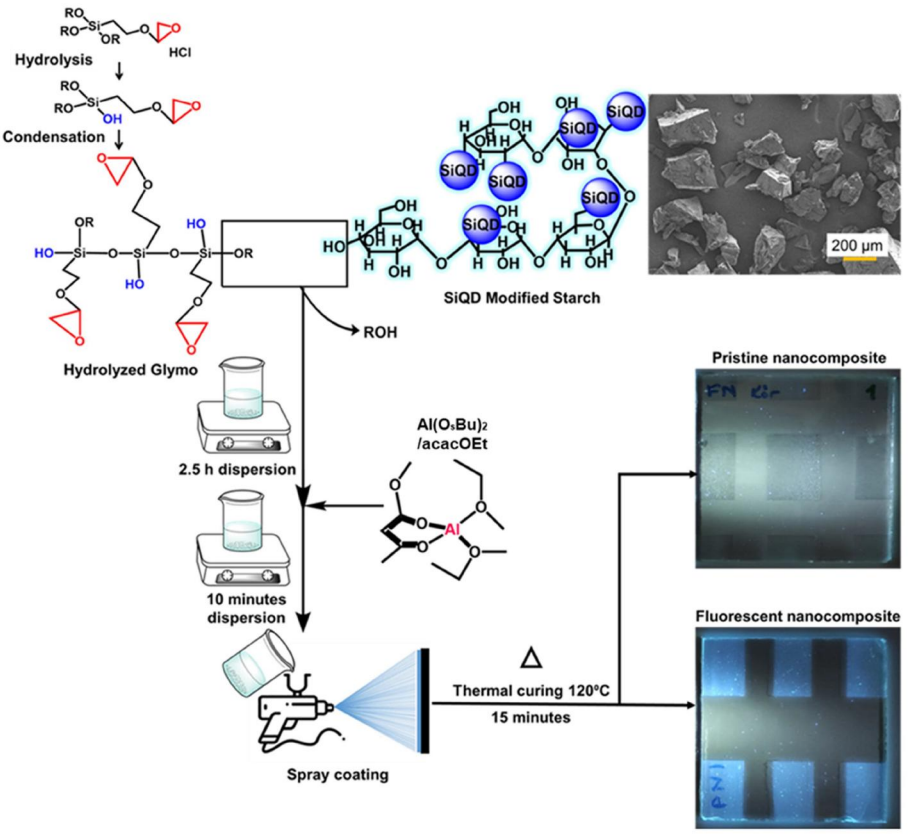

Figure 8. Si QD attached starch embedded inorganic-organic hybrid coating application by spray coating method for the selective regions on the glass substrates for fluorescent applications.

does not contain a similar peak after thermal curing (120 °C, 15 min). SEM figure shows a micron range coating with homogeneous surface characteristics. Additionally, sol-gel polymerization of coated nanocomposite structure monitored by FT-IR and selective area photoluminescence features observed by PL spectroscopy were also presented. PL features (Fig. 9(c)) of blank coating without Si QD-modified starch-embedded nanocomposite structure showed no regular fluorescence. For fluorescent coating, the peak region between 400 and 550 cm^{-1} showed blue-green fluorescence as visually observed (λ_{max} = 485 nm). When F0 and F9 PL features (Supplementary Fig. S8) are compared, it is clear that Si QD attachment provides a regular fluorescent emission, and the intensities are relatively organized with varying excitation values, as observed with Si QD attachments in other examples.[49,50]

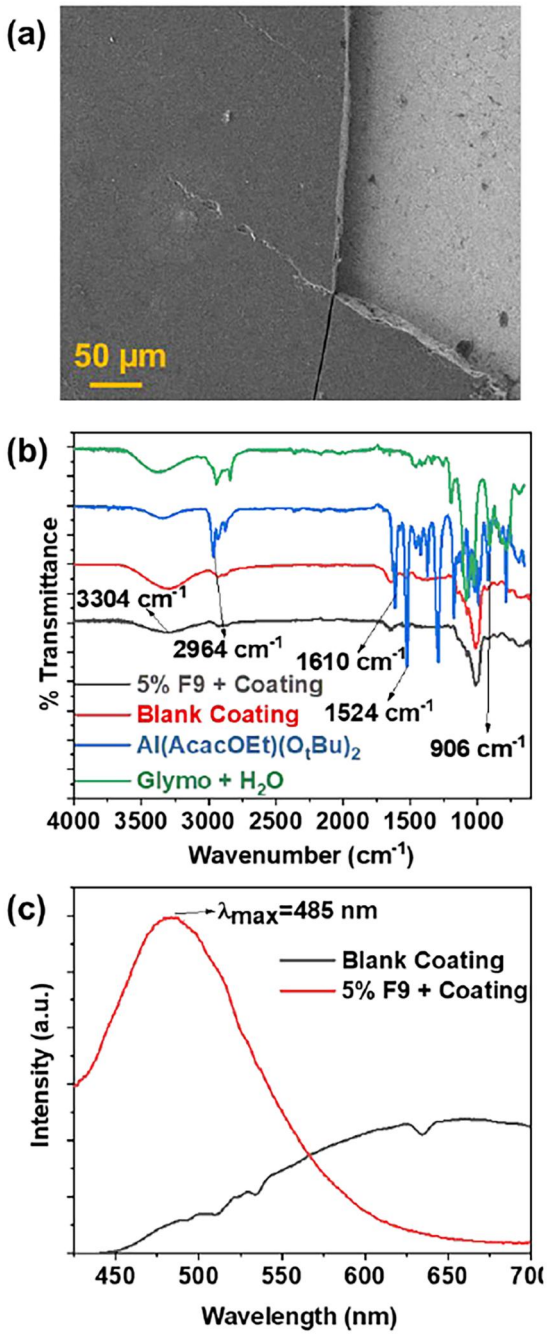

Figure 9. (a) SEM investigation of the Si QD attached starch embedded nanocomposite coating on glass and (b) FT-IR monitoring of the hybrid nanocomposite structure and (c) PL spectrum of the blank and Si QD attached starch embedded nanocomposite coating.

Conclusion

A new technique was developed for covalent attaching of Si QDs to starch particles via sol-gel control. Si QDs were developed with a well-designed QD synthesis method and applied to starch modification. UV treatment provided size-controlled Si QDs, which can be attached to starch molecules. After Si QD attachment, the optical, physical, and mechanical features of starch particles were varied on a molecular level, thus resulting in a new nanocomposite material for fluorescent coating barcode applications. Sol-gel reactions and molecular condensation were studied with FT-IR, XPS, and PL spectroscopy. Also, thermal investigations confirmed the Si QD attachment by specific decomposition peaks. Selected concentrations of Si QDs were investigated separately, and more detailed investigations were performed for each sample. Results showed that XPS and atomic mapping could detect Si QD modification on starch molecules in addition to EDX analysis. The obtained Si QD-modified starch materials were embedded into inorganic–organic nanocomposite coatings on glass for selective fluorescent applications.

Experimental section

Materials

APTES was purchased from Merck. GPTMS was obtained from Degussa, and $Al(OsBu)_3$ was purchased from Fluka. Potato starch and L-AA (99%) were purchased from Sigma-Aldrich. All chemicals were used as received without further purification. UV lamp Osram, Ultravitalux, 300 W and radiated power of 315–400 nm (UVA) at 13.6 W and 280–315 nm (UVB) at 3.0 W were used for Si QD synthesis.

Synthesis and characterization of Si QD-modified starch

The freshly prepared stock solution of L-AA (99%) was mixed with a certain amount of APTES with continuous stirring. Two total solutions were used, 20 and 40 mL, for the Si QD production. The mixtures were homogenized in an ultrasonic bath for 1 min before being placed under UV light (15 cm from the solution, vertical). Different time ranges (30, 45, and 60 min for 20 mL solution and 45, 60, and 75 min for 40 mL solution) of UV treatment were applied (Fig. 1(a–e)).[51,52] Resultant Si QD-modified starches were analyzed using physical and chemical methods to chracterize PL intensity, surface modification, thermal character, and atomic composition. Results were compared to each other to detect the best possible final material for programmable fluorescent applications. Excess amounts of Si QD decoration with inefficient calibers were eliminated, and the total

characteristics of the modified starches were examined. Firstly concentration effect and then time range were systematically evaluated at 80 °C for the formation of the SiQD-modified starch nanocomposite structures.

A comprehensive investigation was conducted for selected products obtained from 20 mL (F9) and 40 mL (F15) of Si QD used to modify starch. We have developed a denotation list for the resultant Si QD modified starches. For example, F1 = UV30 (QD reaction time in minutes spent for the synthesis under UV light)-QD1 (QD number from the list):20 (total volume of primary QD solution)/1(amount in mL used for starch modification), so we denote F1 as UV30-QD1: 20/1. By the same method, F9 is UV60-QD3:20/3, and F15 is UV60-QD5:40/3. Since visible evaluations of the physical features resulted in pale orange-yellow starch after the modification, a perfectly white and pulverized powder product was obtained. In order to produce the white product, heat application was removed, and a low concentration of Si QD (F15 was diluted 50 times) was utilized (F24 is UV60-QD5:40/0.06), leading to the perfect appearance same as the pristine starch.

Additionally, all modified and investigated nanocomposites were compared with pristine starch. Supporting Table S1lists all studies employed with Si QD to modify the starch samples based on the difference in Si QD amount and interaction time. Modifications were performed with 150 mg starch. F24 (UV60-QD5:40/0.06) refers to the modification employed at room temperature.

Modified starch containing fluorescence hybrid nanocomposite structure

Modified starch molecules were utilized to synthesize fluorescence hybrid nanocomposite coating structures. For general fabrication, commercially available GPTMS-Degussa was used as the main sol-gel-based transparent polymeric structure. $Al(OsBu)_3$ was used as a co-reactant after chelation with ethyl acetoacetate (2:3) to control this reactivity since the precursor $Al(OsBu)_3$ is extremely air sensitive. Modified starch molecules F9 were added into the nanocomposite coating solution, and dispersion was applied at about 2.5 h with 2,000 rpm. After the production of the homogeneous mixture, an aluminum complex was added to the solution, and the spray coating technique was selected for the application onto the 10 × 10 cm glass substrates obtained from a local producer. HCl (Merck) and distilled water were used to start the hydrolysis-condensation reactions of GPTMS. Coatings were obtained for selective regions on the glass substrates, showing a fluorescence/glow effect upon fair treatment, whereas coatings with non-modified starch structures reflected no similar behavior.

Characterization of the materials

Si QD were labeled according to the technique presented before. Si QD1, Si QD2, Si QD3 and Si QD4, Si QD5, Si QD6 were presented in Figure S1. TEM, HR-TEM, and UV-Vis spectroscopy results of the synthesized Si QD with 20 and 40 mL precursor solutions were presented in Figure S1. FT-IR-Model (600–4,000 cm^{-1}) was employed to detect specific functional groups such as OH or -NH_2 on Si QD and polymerization behavior of the nanocomposite structure. The shapes and surface characteristics of the pristine starch and modified starch structures were observed with a ZEISS GEMINI 500 SEM machine with Au coating prior to examination. Statistical examination of the sizes of the pristine and Si QD-modified starch structures was obtained by SEM analysis, and the Image J program was applied for each measurement and data collection. The thermal stability features for pristine and Si QD-modified fluorescent starch structures were compared between room temperature and 900 °C with Seiko II brand 7300 TGA-DTA. Atmospheric environments were utilized for the thermal measurements. Crystal structure regimes were examined by XRD (ZEISS GEMINI 500). The surface and elemental composition of the pristine and modified starches were investigated by EDX spectroscopy, and atomic compositions were corrected by the elemental mapping technique performed by the SEM-EDX device. XPS spectra were obtained by a flood gun charge neutralizer system equipped with a monochromated Al Kα X-ray source ($h\nu = 1{,}486.6$ eV), and a 400 mm spot size was applied. Wide energy survey scans were recorded between a binding energy range of 0 and 1,360 eV at a detector pass energy of 200 eV and an energy step size of 1 eV. High-resolution spectra were obtained at a pass energy of 50 eV with energy steps of 0.1 eV for each atom. Photoluminescence analysis for QDs and modified starch brands (PL) was performed with a Horiba Scientific FluoroMax + Spectrofluorometer device with varying excitation and emission characteristics.

Acknowledgments

We gratefully acknowledge Celal Bayar University-DEFAM facilities and Istanbul Sabahattin Zaim University- Halal Food Laboratory. We gratefully acknowledge the TUBITAK BIDEB 2210-A bursary program for its support.

Disclosure statement

No potential conflict of interest was reported by the author(s).

Funding

This paper and project were supported by Istanbul Sabahattin Zaim University, IZU-OGR, and IZU BAP Projects (Project Number: İZÜÖGR-2020-09).

References

[1] Mahmood, K.; Kamilah, H.; Shang, P. L.; Sulaiman, S.; Ariffin, F.; Alias, A. K. A Review: Interaction of Starch/Non-Starch Hydrocolloid Blending and the Recent Food Applications. *Food Biosci.* **2017**, *19*, 110–120. DOI: 10.1016/j.fbio.2017.05.006.

[2] Ellis, R. P.; Cochrane, M. P.; Dale, M. F. B.; Duffus, C. M.; Lynn, A.; Morrison, I. M.; Prentice, R. D. M.; Swanston, J. S.; Tiller, S. A. Starch Production and Industrial Use. *J. Sci. Food Agric.* 1998, *77*(3), 289–311. DOI: 10.1002/(SICI)1097-0010(199807)77:3<289::AID-JSFA38>3.0.CO;2-D.

[3] Whistler, R. L.; BeMiller, J. N.; Paschall, E. F. *Starch: Chemistry and Technology*, 2th ed.; Academic Press: London, 2012.

[4] Krishnan, S.; Kshirsagar, A. C.; Singhal, R. S. The Use of Gum Arabic and Modified Starch in the Microencapsulation of a Food Flavoring Agent. *Carbohydr. Polym.* **2005**, *62*(4), 309–315. DOI: 10.1016/j.carbpol.2005.03.020.

[5] Mourtzinos, I.; Kalogeropoulos, N.; Papadakis, S. E.; Konstantinou, K.; Karathanos, V. T. Encapsulation of Nutraceutical Monoterpenes in β-Cyclodextrin and Modified Starch. *J. Food Sci.* **2008**, *73*(1), 89–94. DOI: 10.1111/j.1750-3841.2007.00609.x.

[6] Maurer, H. W. Starch in the Paper Industry. In *Starch, Edition*; Bemiller, J.; Whistler, R., Eds. Academic Press: New York, 2009; pp. 657–713.

[7] Din, Z.; Chen, L.; Xiong, H.; Wang, Z.; Ullah, I.; Lei, W.; Shi, D.; Alam, M.; Ullah, H.; Khan, S. A. Starch: An Undisputed Potential Candidate and Sustainable Resource for the Development of Wood Adhesive. *Starch* **2020**, *72*(3-4), 1900276. DOI: 10.1002/star.201900276.

[8] Kennedy, H. M. Adhesives from Renewable Resources. In *Starch- and Dextrin-Based Adhesives*; Jessop, J. L. P.; Chan H. W. S., Eds. American Chemical Society: Washington, D.C., 1989; pp 326–336. DOI: 10.1021/bk-1989-0385.ch023.

[9] Whistler, R.L.; Daniel, J.R. Starch. In *Kirk-Othmer Encyclopedia of Chemical Technology*, Othmer, K., Eds. Wiley Blackwell: New Jersey, 2000; pp. 1–15.

[10] Mason, W. R. Starch Use in Foods. In *Starch*, Bemiller, J.; Whistler, R., Eds. 3rd ed.; Academic Press: New York, 2009; pp. 745–795.

[11] Obadi, M.; Xu, B. Review on the Physicochemical Properties, Modifications, and Applications of Starches and Its Common Modified Forms Used in Noodle Products. *Food Hydrocoll.* **2021**, *112*, 106286. DOI: 10.1016/j.foodhyd.2020.106286.

[12] Singh, N.; Kaur, L. Morphological, Thermal, Rheological and Retrogradation Properties of Potato Starch Fractions Varying in Granule Size. *J. Sci. Food Agric.* **2004**, *84*(10), 1241–1252. DOI: 10.1002/jsfa.1746.

[13] Rapaille, A.; Vanhemelrijck, J. *Modified Starches.* In *Thickening and Gelling Agents for Food*, Imeson, A. P., Ed. Springer: Boston, MA, 1997; pp. 199–229.

[14] Kaur, B.; Ariffin, F.; Bhat, R.; Karim, A. A. Progress in Starch Modification in the last decade. *Food Hydrocoll.* **2012**, *26*(2), 398–404. DOI: 10.1016/j.foodhyd.2011.02.016.

[15] Chiu, C. W.; Schiermeyer, E.; Thomas, D. J.; Shah, M. B. Thermally Inhibited Starches and Flours and Process for Their Production. U.S. Patent 5,725,676, March 10, 1998.

[16] Han, Z.; Shi, R.; Sun, D. W. Effects of Novel Physical Processing Techniques on the Multi-structures of Starch. *Trends Food Sci. Technol.* **2020**, *97*, 126–135. DOI: 10.1016/j.tifs.2020.01.006.

[17] Pukkahuta, C.; Shobsngob, S.; Varavinit, S. Effect of Osmotic Pressure on Starch: New Method of Physical Modification of Starch. *Starch Stärke* **2007**, *59*(2), 78–90. DOI: 10.1002/star.200600509.

[18] Masina, N.; Choonara, Y. E.; Kumar, P.; Du Toit, L. C.; Govender, M.; Indermun, S.; Pillay, V. A Review of the Chemical Modification Techniques of Starch. *Carbohydr. Polym.* **2017**, *157*, 1226–1236. DOI: 10.1016/j.carbpol.2016.09.094.

[19] Arslan, O.; Topuz, F.; Eren, H.; Biyikli, N.; Uyar, T. Pd Nanocube Decoration onto Flexible Nanofibrous Mats of Core–Shell Polymer–ZnO Nanofibers for Visible Light Photocatalysis. *New J. Chem.* **2017**, *41*(10), 4145–4156. DOI: 10.1039/C7NJ00187H.

[20] Jobling, S. Improving Starch for Food and Industrial Applications. *Curr. Opin. Plant Biol.* **2004**, *7*(2), 210–218. DOI: 10.1016/j.pbi.2003.12.001.

[21] Keeling, P. L.; Knight, M. E.; Guan, H. Modification of Starch Synthesis in Plants. U.S. Patent 5,824,790, October 20, 1998.

[22] Alfei, S.; Marengo, B.; Zuccari, G. Nanotechnology Application in Food Packaging: A Plethora of Opportunities versus Pending Risks Assessment and Public Concerns. *Food Res. Int.* **2020**, *137*, 109664. DOI: 10.1016/j.foodres.2020.109664.

[23] Chellaram, C.; Murugaboopathi, G.; John, A. A.; Sivakumar, R.; Ganesan, S.; Krithika, S.; Priya, G. Significance of Nanotechnology in Food Industry. *APCBEE Proc.* **2014**, *8*, 109–113. DOI: 10.1016/j.apcbee.2014.03.010.

[24] Kumar, P.; Mahajan, P.; Kaur, R.; Gautam, S. Nanotechnology and Its Challenges in the Food Sector: A Review. *Mater. Today. Chem.* **2020**, *17*, 100332. DOI: 10.1016/j.mtchem.2020.100332.

[25] Wu, J.; Dai, J.; Shao, Y.; Sun, Y. One-Step Synthesis of Fluorescent Silicon Quantum Dots (Si-QDs) and Their Application for Cell Imaging. *RSC Adv.* **2015**, *5*(102), 83581–83587. DOI: 10.1039/C5RA13119G.

[26] Saita, S.; Kawasaki, H. Origin of the Fluorescence in Silica-Based Nanoparticles Synthesized from Aminosilane Coupling Agents. *J. Lumin.* **2021**, *232*, 117849. DOI: 10.1016/j.jlumin.2020.117849.

[27] Jo, S.; Ryu, B.; Chae, A.; Choi, Y.; Kang, E. B.; Nur'aeni; Park, B.; Park, S. Y.; In, I. Microwave-Assisted Synthesis of Highly Fluorescent and Biocompatible Silicon Nanoparticles Using Glucose as Dual Roles of Reducing Agents and Hydrophilic Ligands. *Chem. Lett.* **2017**, *46*(3), 398–400. DOI: 10.1246/cl.161045.

[28] Ddungu, J.; Silvestrini,.; Tassoni, A.; Cola, L. Shedding Light on the Aqueous Synthesis of Silicon Nanoparticles by Reduction of Silanes with Citrates. *Faraday Discuss.* **2020**, *222*(0), 350–361. DOI: 10.1039/C9FD00127A.

[29] Hernández-Abril, P. A.; Iriqui-Razcón, J. L.; León-Sarabia, E.; Leal-Soto, S. D.; Álvarez-Ramos, M. E.; Berman-Mendoza, D.; Higuera-Valenzuela, H. J. Synthesis of Silicon Quantum Dots Using Chitosan as a Novel Reductor Agent. *Rev. Mex. Fís.* **2021**, *67*(2 Mar-Apr), 249–254. DOI: 10.31349/RevMexFis.67.249.

[30] Li, W.; Liu, D.; Dong, D.; You, T. Microwave-Assisted Synthesis of Fluorescent Silicon Quantum Dots for Ratiometric Sensing of Hg (II) Based on the Regulation of Energy Transfer. *Talanta* **2021**, *226*, 122093. DOI: 10.1016/j.talanta.2021.122093.

[31] Oliinyk, B.; Korytko, D.; Lysenko, V.; Alekseev, S. Are Fluorescent Silicon Nanoparticles Formed in a One-Pot Aqueous Synthesis? *Chem. Mater.* **2019**, *31*(18), 7167–7172. DOI: 10.1021/acs.chemmater.9b01067.

[32] Uchino, T.; Kurumoto, N.; Sagawa, N. Structure and Formation Mechanism of Blue-Light-Emitting Centers in Silicon and Silica-Based Nanostructured Materials. *Phys. Rev. B.* **2006**, *73*(23), 233203. DOI: 10.1103/PhysRevB.73.233203.

[33] Zhong, Y.; Peng, F.; Bao, F.; Wang, S.; Ji, X.; Yang, L.; Su, Y.; Lee, S.; He, Y. Large-Scale Aqueous Synthesis of Fluorescent and Biocompatible Silicon Nanoparticles and Their Use as Highly Photostable Biological Probes. *J. Am. Chem. Soc.* **2013**, *135*(22), 8350–8356. DOI: 10.1021/ja4026227.

[34] Tayebi, M.; Tavakkoli Yaraki, M.; Ahmadieh, M.; Mogharei, A.; Tahriri, M.; Vashaee, D.; Tayebi, L. Synthesis, Surface Modification and Optical Properties of Thioglycolic Acid-Capped ZnS Quantum Dots for Starch Recognition at Ultralow Concentration. *J. Electron. Mater.* **2016**, *45*(11), 5671–5678. DOI: 10.1007/s11664-016-4792-y.

[35] Chen, W.; Li, D.; Tian, L.; Xiang, W.; Wang, T.; Hu, W.; Hu, Y.; Chen, S.; Chen, J.; Dai, Z. Synthesis of Graphene Quantum Dots from Natural Polymer Starch for Cell Imaging. *Green Chem.* **2018**, *20*(19), 4438–4442. DOI: 10.1039/C8GC02106F.

[36] Singh, A.; Guleria, A.; Neogy, S.; Rath, M. C. UV Induced Synthesis of Starch Capped CdSe Quantum Dots: Functionalization with Thiourea and Application in Sensing Heavy Metals Ions in Aqueous Solution. *Arabian J. Chem.* **2020**, *13*(1), 3149–3158. DOI: 10.1016/j.arabjc.2018.09.006.

[37] Liu, C.; Liu, Y.; Deng, H.; Tang, S.; Cao, Y. C. High Quantum Yield and Well-Dispersed Quantum Dots Luminescent Composite through Sodium Carboxymethyl Starch. *Luminescence* **2019**, *34*(2), 200–204. DOI: 10.1002/bio.3594.

[38] Staroszczyk, H.; Ciesielski, W.; Tomasik, P. Starch–Metal Complexes and Metal Compounds. *J. Sci. Food Agric.* **2018**, *98*(8), 2845–2856. DOI: 10.1002/jsfa.8820.

[39] Al-Douri, Y.; Badi, N.; Voon, C. H. Synthesis of Carbon-Based Quantum Dots from Starch Extracts: Optical Investigations. *Luminescence* **2018**, *33*(2), 260–266. DOI: 10.1002/bio.3408.

[40] Liu, X.; Zheng, J.; Yang, Y.; Chen, Y.; Liu, X. Preparation of N-Doped Carbon Dots Based on Starch and Their Application in White LED. *Opt. Mater.* **2018**, *86*, 530–536. DOI: 10.1016/j.optmat.2018.10.057.

[41] Yan, Z.; Shu, J.; Yu, Y.; Zhang, Z.; Liu, Z.; Chen, J. Preparation of Carbon Quantum Dots Based on Starch and Their Spectral Properties. *Luminescence* **2015**, *30*(4), 388–392. DOI: 10.1002/bio.2744.

[42] Liu, Y.; Yang, L.; Ma, C.; Zhang, Y. Thermal Behavior of Sweet Potato Starch by Non-Isothermal Thermogravimetric Analysis. *Materials* **2019**, *12*(5), 699. DOI: 10.3390/ma12050699.

[43] Wang, S.; Hu, X.; Wang, Z.; Bao, Q.; Zhou, B.; Li, T.; Li, S. Preparation and Characterization of Highly Lipophilic Modified Potato Starch by Ultrasound and Freeze-Thaw Treatments. *Ultrason. Sonochem.* **2020**, *64*, 105054. DOI: 10.1016/j.ultsonch.2020.105054.

[44] dos Santos, T. P. R.; Leonel, M.; Garcia, É. L.; do Carmo, E. L.; Franco, C. M. L. Crystallinity, Thermal and Pasting Properties of Starches from Different Potato Cultivars Grown in Brazil. *Int. J. Biol. Macromol.* **2016**, *82*, 144–149. DOI: 10.1016/j.ijbiomac.2015.10.091.

[45] Peidayesh, H.; Ahmadi, Z.; Khonakdar, H. A.; Abdouss, M.; Chodák, I. Fabrication and Properties of Thermoplastic Starch/Montmorillonite Composite Using Dialdehyde Starch as a Crosslinker. *Polym. Int.* **2020**, *69*(3), 317–327. DOI: 10.1002/pi.5955.

[46] Qiang, R.; Yang, S.; Hou, K.; Wang, J. Synthesis of Carbon Quantum Dots with Green Luminescence from Potato Starch. *New J. Chem.* **2019**, *43*(27), 10826–10833. DOI: 10.1039/C9NJ02291K.

[47] Arslan, O.; Arpaç, E.; Sayılkan, F.; Sayılkan, H. Hybrid Sol–Gel Coating on Al. *J. Mater. Sci.* **2007**, *42*(6), 2138–2142. DOI: 10.1007/PL00021937.

[48] Arslan, O.; Arpac, E.; Sayılkan, H. Siliconcarbide Embedded Hybrid Nanocomposites as Abrasion Resistant Coating. *J. Inorg. Organomet. Polym.* **2010**, *20*(2), 284–292. DOI: 10.1007/s10904-010-9360-y.

[49] Arslan, O.; Singh, A. P.; Belkoura, L.; Mathur, S. Cysteine-Functionalized Zwitterionic ZnO Quantum Dots. *J. Mater. Res.* **2013**, *28*(14), 1947–1954. DOI: 10.1557/jmr.2013.161.

[50] Arslan, O.; Belkoura, L.; Mathur, S. Swift Synthesis, Functionalization and Phase-Transfer Studies of Ultrastable, Visible Light Emitting Oleate@ ZnO Quantum Dots. *J. Mater. Chem. C.* **2015**, *3*(45), 11965–11973. DOI: 10.1039/C5TC03377B.

[51] Arslan, O.; Aytac, Z.; Uyar, T. Fluorescent Si QD Decoration onto a Flexible Polymeric Electrospun Nanofibrous Mat for the Colorimetric Sensing of TNT. *J. Mater. Chem. C.* **2017**, *5*(7), 1816–1825. DOI: 10.1039/C6TC05521D.

[52] Arslan, O.; Uyar, T. Multifunctional Electrospun Polymeric Nanofibrous Mats for Catalytic Reduction, Photocatalysis and Sensing. *Nanoscale* **2017**, *9*(27), 9606–9614. DOI: 10.1039/C7NR02658G.